Available online at www.sciencedirect.com

ScienceDirect

Procedia Manufacturing 48 (2020) 737–742

Procedia MANUFACTURING

www.elsevier.com/locate/procedia

48th SME North American Manufacturing Research Conference, NAMRC 48 (Cancelled due to COVID-19)

Effect of in-process laser interface heating on strength isotropy of extrusion-based additively manufactured PEEK

Pu Han, Alireza Tofangchi, Sihan Zhang, Anagh Desphande, Keng Hsu *

J. B. Speed School of Engineering, University of Louisville, Louisville, USA

* Corresponding author. Tel.: 502-852-8616; fax: 502-852-8616. E-mail address: Keng.Hsu@louisville.edu

Abstract

Fused Filament Fabrication (FFF) 3D printing provides an effective solution for fabrication of custom components at affordable cost and in short time. Nevertheless, relative to the conventional methods, the anisotropic properties exhibited by FFF 3D printed parts cause the mechanical strength to be less satisfactory. In order to resolve the problem, we propose an in-process laser local pre-deposition heating (LLPH) method, which is capable of enhancing thermal relaxation at inter-layer interface and reinforcing inter-layer adhesion, that ultimately resulted in an increase in tensile strength along the build direction. This improvement in tensile strength of the build parts with in-process laser power has been demonstrated in this manuscript. Besides, the subsequent relevance with polymer relaxation, reptation and entanglement has been discussed. As verified by mechanical testing, tensile strength was improved by 350% compared to control sample and 99.5% isotropy was achieved (build-direction strength divided by in-plane strength) with the application of laser. Scanning Electron Microscope was used to make observation of isotropic behavior at inter-layer interface.

Keywords: Additige manufacturing; Laser assisted process; Inter-layer strength; PEEK; Reptation

1. Introduction

The Fused filament fabrication (FFF) has turned out to be one of the desired method for thermal plastic additive manufacturing due to its flexibility, capability and cost-effectiveness [1]. Thermoplastic filaments are taken as the starting material during the process. After being extruded through a heated nozzle, the filament is kept nearly above the glass transition temperature of the thermoplastic polymer filament. Then, it undergoes the process of direct deposition and layer-by-layer construction of a 3D component [2]. Utilizing a slicing software to control process parameters such as density and inner support pattern, the fabrication of components with complex shapes can be easily achieved [3]. Despite multitude of advantages [4] as well as the capability to print various applicable materials; i.e. amorphous polymers like acrylonitrile butadiene styrene [4], polycarbonate [5] and semi-crystalline polymer like poly-lactic acid [6], FFF still suffers from several shortcomings. For instance, the parts fabricated by this method possess poor mechanical strength, especially in the build direction, in contrast to those manufactured with traditional methods. Moreover, the mechanical properties exhibited by FFF-3D printed parts are anisotropic [7].

In order for resolving the mechanical property anisotropy in FFF-printed parts, optimizing process parameters (such as nozzle temperature, layer thickness, raster strategy and air gap), ultrasound based techniques [8–13] and use of statistical analysis tools (design of experiments [14–16], Taguchi method [17–20], fuzzy logic [21] and parameter investigation [22,23]) have been the major thrust in the literature. With regard to these approaches, the current major shortcoming is a trade-off between different process parameters for the purpose of reaching the maximum inter-layer strength. However, the fundamental physics governing the inter-layer bond formation mechanism remain unresolved. According to some other

10.1016/j.promfg.2020.05.107

methods, the mechanical properties possessed by FFF printed components could be improved by; for instance, printing in vacuum to mitigate the heat losses and porosity induced by conduction [24], ultrasound-assisted printing [13], printing in low oxygen environment [25] or carrying out thermal treatment subsequent to processing [26].

At the microstructure level, the motion of polymer chains across the interface between layers is what the inter-layer strength of FFF components is reliant on. Based on reptation model, polymer chains are capable of moving towards one end if the temperature exceeds glass transition temperature. This motion of polymer chains is called reptation [27,28]. Therefore, the increase in polymer reptation makes it easier for the interfacial bond strength to be improved by raising print temperature [29]. Nevertheless, if temperature is in excess of a certain limit, degradation happens [30]. Additionally, it is proven that weld strength is associated with welding time as a function of $t^{1/4}$ prior to a full entanglement of polymer in the weld region [31–35]. In numerous investigations, the focus was placed on the melting behavior of polymer diffusion in equilibrium state [36,37], while later it was discovered that the transient behavior of the polymer melt is equally significant to the development of ultimate microstructure as well. Taking these factors into consideration, a method could be proposed to ensure effective improvement to mechanical strength; that is, the direct introduction of heat to the inter-layer interface over the course of printing.

Previously, an in-process laser pre-deposition heating technique with near-infrared laser was reported for heating of the interface between current and the previous layers ahead of nozzle path. In comparison to control samples (samples printed without laser pre-deposition), the bonding strength (in bending test) was improved by 77% in FFF-printed ABS material [38,39]. The work was further improved to reach 83% tensile strength of that along in-plane direction, using a 10.6 μm infrared CO_2 laser with Ultem 1010 [40].

In this study, to facilitate FFF-3D printing of PEEK by CO_2 infrared laser, a redesigned and optimized technique was applied. A comparison is performed with tensile strength of horizontal control samples (samples tested along the printed track direction), vertical control sample (samples tested perpendicular to track direction), laser pre-deposition heating samples and filament feedstock. In addition, an analysis is presented to probe failures at inter-layer interface as well as over cross-section. A scalable approach was devised to produce nearly isotropic parts by using these results along with supporting evidence of improved reptation and entanglement across the interfaces.

2. Experimental

2.1. Localized laser pre-heating apparatus

A high temperature printing system with laser pre-deposition heating process was built with a closed-chamber 3D printer (Funmat HT, Intamsys, Shanghai, China) along with the laser components. As shown in Fig. 1, first, a laser beam was generated by a 10.6 μm CO_2 Laser. This beam then was coupled by a laser coupler into an optical fiber which was focused by a laser collimator to a spot-reflected using a gold mirror at a 2 mm distance away (edge of beam to edge of nozzle) from nozzle on the previously printed layer. Specifications of optical parts used are shown in Table 1. The focused beam spot was oval-shaped with a size of 4 mm and 2.5 mm in length and width, respectively. The laser collimator and gold mirror were held by a bracket that was installed on the extruder, allowing the laser spot to travel with the extruder and to stay focused on the previously printed layer while the extruder moves from left to the right. The bracket is designed to hold 4 laser collimators and 4 gold mirrors along 4 directions in x-y plane (+x, -x, +y, -y). In this work, laser along +x direction is used for all the prints. It is worth noting that since laser collimator was installed and held vertically in the new design, the loss of printable area due to additional laser apparatus significantly reduced compared to that in previous setting [40].

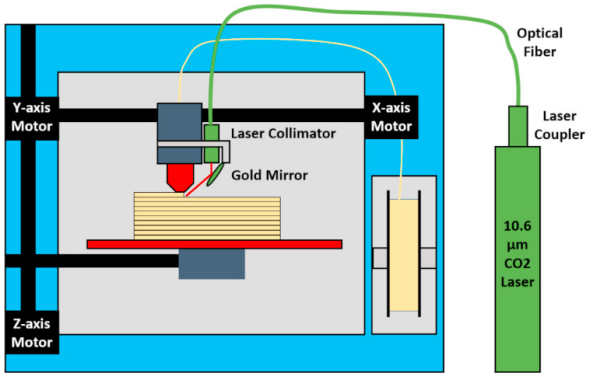

Fig. 1. Schematic diagram of experimental set for FFF printing using pre-deposition laser heating.

Table 1. Specifications of laser components.

Component	Make/Shape	Specifications
Laser Source	Synrad 48-1KAN (Mukilteo, USA)	Wavelength:10.6 μm, Power: 30W max
Coupler	Laser Component (Bedford, USA)	Energy loss <1dB
Optical fiber	Polymicro (Phoenix, USA)	Length: 2 meters, $< 1dB/meter$
Collimator	Laser Component (Bedford USA)	Focal Length:25.4 mm, Diameter:19mm
Focused laser	Elliptical	Size: 4mm*2.5mm

2.2. Sample preparation

All prints were fabricated using high temperature 3D printing system with laser pre-deposition heating introduced above. There are two categories of samples prepared, control and laser samples, prepared without and with laser pre-deposition heating, respectively. The tensile strengths of laser samples (z-direction, for inter-layer strength) were compared to that of control samples along both build direction (z-direction, for inter-layer strength, vertical control sample) and in-plane direction (x-direction, for inner-layer strength, horizontal control sample).

The printer is controlled by G-codes generated in Intamsys slicing software. A 0.4 mm (that is commonly used in commercial 3D printer) E3D stainless steel volcano nozzle was used for all prints in this work. 380 ℃ nozzle temperature, 150 ℃ build plate temperature, and 90 ℃ ambient temperature were maintained for all builds based on manufacture recommendations and parameter space investigation. Other process parameters were shown in Table 2. Homogeneous PEEK (3DXTech, Grand Rapids, USA) was used as the filament feedstock. Filament specification given by 3DXTech is shown in Table 3. In order to avoid the influence of humidity, the filament was kept in a furnace at 100 ℃ for dehydration overnight. Before printing, Uline silica gel desiccant was used to maintain low humidity in filament chamber during print and a hygrometer (Thermo Pro TP50, Thermo, Toronto, Canada) was used to ensure consistent low humidity being maintained inside the chamber for all prints.

Table 2. FFF process parameters.

Parameter	Data
Pattern shown in Fig. 2 (a)	Single wall
Layer height	0.2mm
Extrusion width	1mm
Extrusion temperature	380 ℃
Bed temperature	150 ℃
Environment temperature	80 ℃
Print speed	10 mm/s
Raft	Yes

Table 3. PEEK filament specification.

Specification	Data
Glass transition temperature	143 ℃
Diameter	1.75 mm (+/- 0.05 mm)
Density	1.3 g/cc
Color	Natural/Tan
Tensile strength	100 MPa
Recommended Extrude Temperature	375 - 410 ℃
Recommended Bed temperature	130 - 145 ℃
Recommended Print speed	10 – 50 mm/s

The part printed was a single-wall hollow rectangular box, 100 mm long, 13 mm wide and 20 mm-tall with two semi-circular ends is shown in Fig.2 (a). A raft was used for the base. The longer side of the box was along x-axis to match the direction of laser focused spot as shown in Fig. 1. During raft print, laser was turned on and maintained at 0% output power for warmup, then gradually increased using power knob to the final power level (in percentage of laser power) when raft was finished. The output power was measured using a Power meter (Thorlabs, Newton, US). The box was printed layer by layer with a 0.2 mm layer height and 1 mm width. It is important to notice that only front side of the box, where nozzle moves from left to right, was pre-deposition heated while the backside of the wall was post-deposition heated. After print, the box was removed from build plate immediately and cooled down to the room temperature outside the chamber.

A rotary cutter (Dremel, Mount Prospect, US) with 0.5 mm thick diamond wheel was used to cut the rectangular box into flat wall shapes to be used in milling machine, since printed PEEK was too brittle to be cut using wire cutter. Only the front side (where pre-deposition heating occurred) was used for tests. A desktop PCB milling machine was used to mill samples into tensile bars. Seven tensile bars can be milled out from each cut wall. Shape and size of one sample tensile bar is shown in Fig.2 (b).

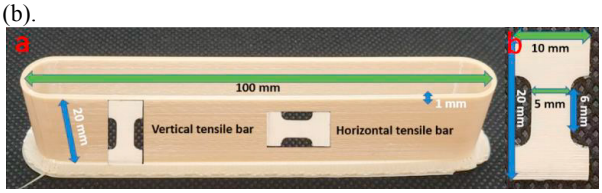

Fig. 2. (a) Single wall rectangular box (5 samples each set); (b) Machined tensile bar.

2.3. Mechanical testing-tensile strength

MTI-2K tensile testing machine (Measurements Technology Inc. Marietta, US) was used to test PEEK tensile bars. Out of seven samples cuts from left to right, the 5 middle tensile bars machined from each set were used for testing and the last two tensile bars in each set were used as replacement of error data, i.e. samples that broke by metal clip on tensile tester. A pre-load of 3 N was used and pulling speed was set to be 5 mm/s. Ultimate tensile strength was used as reference for all tensile bars.

3. Result and discussion

Tensile strength data of laser pre-deposition heating PEEK samples (along the build direction, red dots), horizontal control samples (Control H), and vertical control samples (Control V) are shown in Fig. 3. The average (red dot) and standard deviation (error bar) were calculated from 5 samples in each set. The straight line for horizontal control sample and vertical control sample are averages of 5 samples as well. From Fig. 3, laser pre-deposition heating increased inter-layer bonding strength by a factor greater than 4 (increase of 350%), from 17.8 MPa to 80.4 MPa at 2.13 W of laser power. Of particular interest, the laser sample (at 2.13 W) shows 99.5% tensile strength compared to that of horizontal control sample with the standard deviation of 3.7%. Along with this investigation, the SEM image also revealed further details of fracture propagation at tensile test as shown in Fig. 4 (b). It is evident from these images that the fracture surfaces in laser samples extend inside layers, while fracture surface of vertical control samples stopped at the layer interface and did not progress inside the layers. Thus, it can be confidently concluded that the laser pre-deposition heating has increased the bonding strength at the interface to as strong as the material strength (strength of extruded filament feedstock).

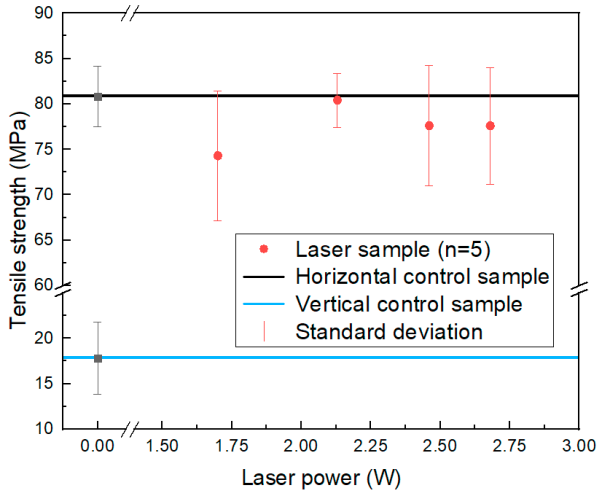

Fig. 3. Tensile strength of laser pre-deposition heating PEEK tensile bar and control samples.

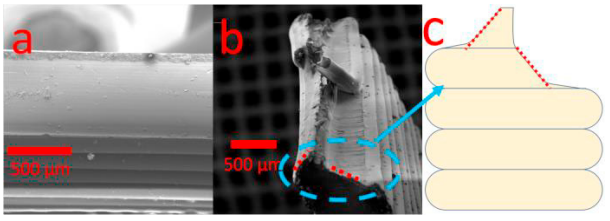

Fig. 4. SEM of tensile test failure surface for (a) Vertical control sample; (b) 2.13 W laser sample. (c) the schematic (side view) of fracture surface progression

Note that tensile strengths for vertical control samples, horizontal control samples and 3DXTech data (shown in Tab. 3) are 17.8 MPa, 80.8 MPa and 100 MPa, respectively. Hence, there has been 19.2% tensile strength loss with respect to original material through the printed track. This strength loss is highly likely caused by shear flow in the nozzle, which elaborated in rheological model in [41]. Briefly, in this model, shear force applied to polymer within the nozzle is a function of flow rate and distance from the nozzle wall. The nozzle shear force, in essence, induces stretch and disentanglement to polymer chains, which ultimately give rise a reduction in mechanical strength of the material.

In order to increase inter-layer reptation, laser pre-deposition heating was used to increase the interface temperature, which expected to increase reptation and relaxation at the inter-layer interface as shown in the conceptual drawing in Fig. 5. The relationship between the interlayer strength and the mass transfer and microstructure of polymer can be described by the relationship proposed by Ezekoye [35].

$$\frac{\sigma_t}{\sigma_{max}} = \left(\frac{t_{weld}}{\tau_{rep}}\right)^{1/4} = \left(\frac{t_{weld} D_s}{R_g^2}\right)^{1/4} \quad (1)$$

where σ_t, σ_{max} are the strength of the interface and the tensile strength of the material respectively, t_{weld} is the healing time of the interface(or time during which the interface stays above glass transition or melting temperature), τ_{rep} is the reptation time, D_s is the center of mass diffusivity of polymer chains, and R_g is the radius of gyration of polymer chains.

In this work, it is hypothesized that laser was used to increase interface temperature yet below the threshold of degradation limit, which is expected to give rise longer reptation time to reach a high percentage of isotropic microstructure. As a result, tensile strength of laser pre-deposition heating sample reached 99.5% that of horizontal control sample (breaking polymer chains). As shown in Fig.4 (b), the fracture trajectory starts from the edge and breaks into layer and ends up with a curved surface that extends to an upper layer at the center. Parts of this behavior may be attributed to the fact that the longer edge of the track was exposed to air, hence cooled down faster than that in the center, i.e. allowing less time for relaxation and reptation. As the crack edge moves from the side interface towards center, it fairly shows a 45-degree inclination, perhaps due to ductile fracture in shear mode.

The average tensile strength increased with laser power until the degradation temperature was reached (575 - 580 ℃) [42]. As shown in Fig. 3, the tensile strength of PEEK laser sample increased until 2.13 W, after which it began to decline in the range between 2.13 W and 2.97 W due to polymer degradation.

It is hypothesized that nearly all polymer chains are highly stretched and disentangled. Thus, in order for the printed polymer to recover to isotropic status, the polymer chains need to recover from the residual stresses induced by nozzle flow and 90 ° turn, and reptate as far as the radius of gyration. The conceptual drawing of initial state is shown in Fig. 5 (a), where the red curve represents a polymer chain at bottom of upper layer, and the blue curve represents a polymer chain at top of lower layer. Both polymer chains are highly stretched (not in cluster shape). The polymer relaxation and reptation are two of key elements playing role in constructing interlayer adhesion independently, despite both are function of temperature. Through relaxation, the polymer chains tend to undergo a spring back to its original length with subsequent reduction of residual stress (Fig. 5 (b)). The reptation however is tendency of the polymer chains to slide along with a possibility of crossing the inter-layer interface to entangle with polymer chains in the other layer. The driving force for reptation is thermal diffusion and chain geometry (D_s, R_g) while that for the relaxation is rheology, i.e. polymer viscoelastic properties. Previous studies [43] found out sufficient time above glass transition temperature needs to be given in order to obtain isotropic property in regular 3D printing parts (as predicted in Equation above). This outcome however will not fully occur in reality, possibly due to missing effect of relaxation and entanglement in as other factors affecting in forming interlayer adhesion.

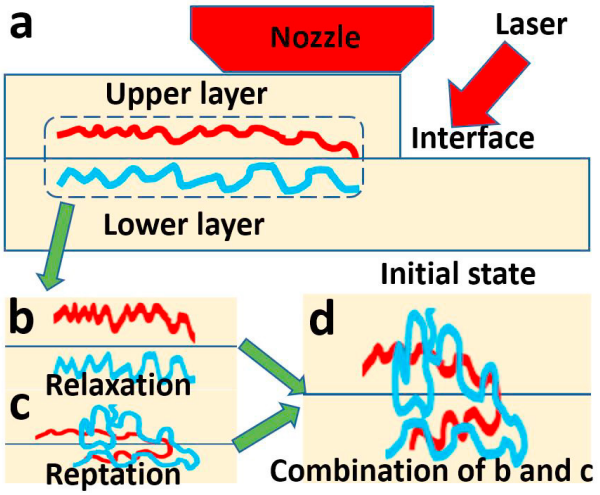

Fig. 5. Schematic diagram of Reptation and Relaxation(a) Initial state: stretched and disentangled; (b) Relaxation only; (c) Reptation only; (d) Combination of relaxation and reptation.

4. Conclusion

This work presents the effect of laser pre-deposition heating on tensile strength and tensile fracture behavior of FFF-printed PEEK. Tensile strength of laser pre-heated sample at 2.13 W reaches 80.4 MPa, which is 99.5% of that in in-plane direction, equivalent to 350.9% increase compared to control sample along build direction. The higher temperature exposure of layer interface and increased time dependent relaxation led to a marked increase in inter-layer bonding strength. Based on indirect evidence, it was speculated that the rising level of inter-layer strength can be attributed to the healing of the interface, which is driven by increased reptation and entanglement of polymer chains under the context of laser pre-deposition heating. Based on these results, laser pre-deposition heating is considered as a viable means of improving the built-part isotropy and their mechanical strength to enhance the extrusion-based polymer 3D printing processes.

References

[1] B. Brenken, E. Barocio, A. Favaloro, V. Kunc, R.B. Pipes, Fused filament fabrication of fiber-reinforced polymers: A review, Addit. Manuf. 21 (2018) 1–16.

[2] B. Stucker, I. Gibson, D. Rosen, Additive Manufacturing Technologies, Springer. (2010).

[3] L. Li, Q. Sun, C. Bellehumeur, P. Gu, Composite modeling and analysis for fabrication of FDM prototypes with locally controlled properties, J. Manuf. Process. 4 (2002) 129–141.

[4] B. N. Turner, R. Strong, S. A. Gold, A review of melt extrusion additive manufacturing processes: I. Process design and modeling, Rapid Prototyp. J. 20 (2014) 192–204.

[5] N. Hill, M. Haghi, Deposition direction-dependent failure criteria for fused deposition modeling polycarbonate, Rapid Prototyp. J. 20 (2014) 221–227.

[6] D. Drummer, S. Cifuentes-Cuéllar, D. Rietzel, Suitability of PLA/TCP for fused deposition modeling, Rapid Prototyp. J. 18 (2012) 500–507.

[7] C. Ziemian, M. Sharma, S. Ziemian, Anisotropic mechanical properties of ABS parts fabricated by fused deposition modelling, in: Mech. Eng., InTech, 2012.

[8] R. Anitha, S. Arunachalam, P. Radhakrishnan, Critical parameters influencing the quality of prototypes in fused deposition modelling, J. Mater. Process. Technol. 118 (2001) 385–388.

[9] K. Thrimurthulu, P.M. Pandey, N.V. Reddy, Optimum part deposition orientation in fused deposition modeling, Int. J. Mach. Tools Manuf. 44 (2004) 585–594.

[10] B.H. Lee, J. Abdullah, Z.A. Khan, Optimization of rapid prototyping parameters for production of flexible ABS object, J. Mater. Process. Technol. 169 (2005) 54–61.

[11] G.P. Kumar, S.P. Regalla, Optimization of support material and build time in fused deposition modeling (FDM), in: Appl. Mech. Mater., Trans Tech Publ, 2012: pp. 2245–2251.

[12] F. Rayegani, G.C. Onwubolu, Fused deposition modelling (FDM) process parameter prediction and optimization using group method for data handling (GMDH) and differential evolution (DE), Int. J. Adv. Manuf. Technol. 73 (2014) 509–519.

[13] A. Tofangchi, P. Han, J. Izquierdo, A. Iyengar, K. Hsu, Effect of Ultrasonic Vibration on Interlayer Adhesion in Fused Filament Fabrication 3D Printed ABS, Polymers (Basel). 11 (2019) 315.

[14] D. Horvath, R. Noorani, M. Mendelson, Improvement of surface roughness on ABS 400 polymer using design of experiments (DOE), in: Mater. Sci. Forum, Trans Tech Publ, 2007: pp. 2389–2392.

[15] K. Chin Ang, K. Fai Leong, C. Kai Chua, M. Chandrasekaran, Investigation of the mechanical properties and porosity relationships in fused deposition modelling-fabricated porous structures, Rapid Prototyp. J. 12 (2006) 100–105.

[16] T. Nancharaiah, Optimization of process parameters in FDM process using design of experiments, Int J Emerg Technol. 2 (2011) 100–102.

[17] C. Chung Wang, T.-W. Lin, S.-S. Hu, Optimizing the rapid prototyping process by integrating the Taguchi method with the Gray relational analysis, Rapid Prototyp. J. 13 (2007) 304–315.

[18] A.K. Sood, R.K. Ohdar, S.S. Mahapatra, Improving dimensional accuracy of fused deposition modelling processed part using grey Taguchi method, Mater. Des. 30 (2009) 4243–4252.

[19] J.W. Zhang, A.H. Peng, Process-parameter optimization for fused deposition modeling based on Taguchi method, in: Adv. Mater. Res., Trans Tech Publ, 2012: pp. 444–447.

[20] J. Laeng, Z.A. Khan, S.Y. Khu, Optimizing flexible behaviour of bow prototype using Taguchi approach, J. Appl. Sci. 6 (2006) 622–630.

[21] R.K. Sahu, S.S. Mahapatra, A.K. Sood, A study on dimensional accuracy of fused deposition modeling (FDM) processed parts using fuzzy logic, J. Manuf. Sci. Prod. 13 (2013) 183–197.

[22] A.K. Sood, R.K. Ohdar, S.S. Mahapatra, Parametric appraisal of mechanical property of fused deposition modelling processed parts, Mater. Des. 31 (2010) 287–295.

[23] Y. Zhang, K. Chou, A parametric study of part distortions in fused deposition modelling using three-dimensional finite element analysis, Proc. Inst. Mech. Eng. Part B J. Eng. Manuf. 222 (2008) 959–968.

[24] H.J. O'Connor, D.P. Dowling, Evaluation of the influence of low pressure additive manufacturing processing conditions on printed polymer parts, Addit. Manuf. 21 (2018) 404–412.

[25] F. Lederle, F. Meyer, G.-P. Brunotte, C. Kaldun, E.G. Hübner, Improved mechanical properties of 3D-printed parts by fused deposition modeling processed under the exclusion of oxygen, Prog. Addit. Manuf. 1 (2016) 3–7.

[26] J. Torres, J. Cotelo, J. Karl, A.P. Gordon, Mechanical property optimization of FDM PLA in shear with multiple objectives, Jom. 67 (2015) 1183–1193.

[27] S.-H. Ahn, M. Montero, D. Odell, S. Roundy, P.K. Wright, Anisotropic material properties of fused deposition modeling ABS, Rapid Prototyp. J. 8 (2002) 248–257.

[28] S.H. Masood, K. Mau, W.Q. Song, Tensile properties of processed FDM polycarbonate material, in: Mater. Sci. Forum, Trans Tech Publ, 2010: pp. 2556–2559.

[29] Q. Sun, G.M. Rizvi, C.T. Bellehumeur, P. Gu, Effect of processing conditions on the bonding quality of FDM polymer filaments, Rapid Prototyp. J. 14 (2008) 72–80.

[30] I. Gibson, D.W. Rosen, B. Stucker, Design for additive manufacturing, in: Addit. Manuf. Technol., Springer, 2010: pp. 299–332.

[31] K. Jud, H.H. Kausch, J.G. Williams, Fracture mechanics studies of crack healing and welding of polymers, J. Mater. Sci. 16 (1981) 204–210.

[32] D.B. Kline, R.P. Wool, Polymer welding relations investigated by a lap shear joint method, Polym. Eng. Sci. 28 (1988) 52–57.

[33] R. Schnell, M. Stamm, C. Creton, Mechanical properties of homopolymer interfaces: Transition from simple pullout to crazing with increasing interfacial width, Macromolecules. 32 (1999) 3420–3425.

[34] P.-G. De Gennes, Introduction to polymer dynamics, CUP Archive, 1990.

[35] O.A. Ezekoye, C.D. Lowman, M.T. Fahey, A.G. Hulme-Lowe, Polymer weld strength predictions using a thermal and polymer chain diffusion analysis, Polym. Eng. Sci. 38 (1998) 976–991.

[36] R.P. Wool, K.M. O'connor, A theory crack healing in polymers, J. Appl. Phys. 52 (1981) 5953–5963.

[37] T. Ge, F. Pierce, D. Perahia, G.S. Grest, M.O. Robbins, Molecular dynamics simulations of polymer welding: Strength from interfacial entanglements, Phys. Rev. Lett. 110 (2013) 98301.

[38] A. Deshpande, A. Ravi, S. Kusel, R. Churchwell, K. Hsu, Interlayer thermal history modification for interface strength in fused filament fabricated parts, Prog. Addit. Manuf. (2018) 1–8.

[39] A.K. Ravi, A. Deshpande, K.H. Hsu, An in-process laser localized pre-deposition heating approach to inter-layer bond strengthening in extrusion based polymer additive manufacturing, J. Manuf. Process. 24 (2016) 179–185.

[40] P. Han, A. Tofangchi, A. Deshpande, S. Zhang, K. Hsu, An approach to improve interface healing in FFF-3D printed Ultem 1010 using laser pre-deposition heating, Procedia Manuf. 34 (2019) 672–677.

[41] C. McIlroy, P.D. Olmsted, Deformation of an amorphous polymer during the fused-filament-fabrication method for additive manufacturing, J. Rheol. (N. Y. N. Y). 61 (2017) 379–397.

[42] H. Zhang, Fire-safe polymers and polymer composites, Office of Aviation Research, Federal Aviation Administration, 2004.

[43] C. McIlroy, P.D. Olmsted, Disentanglement effects on welding behaviour of polymer melts during the fused-filament-fabrication method for additive manufacturing, Polymer (Guildf). 123 (2017) 376–391.